

Application of remote monitoring of biosignals and geolocation with a wearable for patients with sequelae of the coronavirus

Santiago Linder Rubiños Jimenez¹, Mario Alberto Garcia Perez¹, Eduardo Nelson Chavez Gallegos¹, Linett Angélica Velasquez Jimenez², Niko Alain Alarcon Cueva¹, Mauro Bernardo Sanchez Cabrera¹

¹Department of Electrical Engineering, Faculty of Electrical and Electronic Engineering (FIEE), Universidad Nacional del Callao (UNAC), Callao, Peru

²Department of Industrial Engineering, Faculty of Industrial Engineering and Systems (FIIS), Universidad Nacional del Callao (UNAC), Callao, Peru

Article Info

Article history:

Received May 30, 2023

Revised Aug 11, 2023

Accepted Oct 25, 2023

Keywords:

Biosignals
Internet of things
MIT APP inventor
Post-COVID-19
Wearable

ABSTRACT

Several patients who have overcome coronavirus disease (COVID-19) have been left with cardiovascular and pulmonary sequelae and most medical centers lack a remote monitoring system for each patient that notifies them of any complications during rehabilitation. The objective of this research was to implement a wearable that monitors the patient's health and alerts in case of detecting any anomaly. For this reason, a wearable was developed that displays the patient's heart rate, oxygen saturation (SpO₂) level and body temperature on the light emitting diode (LCD) and the application mobile, sending an alert and geolocation message if anomalies are detected in vital signs. The standard deviation of heart rate, temperature and SpO₂ was obtained, which was 1.4930, 0.1558, and 0.4364 in the rest stage, respectively, and 6.3442, 0.2365, and 0.9186 in the physical activity stage respectively with a maximum duration of 42 hours and 52 minutes of battery, managing to send alert messages and store the information in the cloud, which allows to conclude that the wearable can facilitate the management of the database and the location of the patient, that the measurement error increases with physical activity, and that battery life varies with the number of biosignal readings per hour.

This is an open access article under the [CC BY-SA](https://creativecommons.org/licenses/by-sa/4.0/) license.



Corresponding Author:

Eduardo Nelson Chavez Gallegos

Department of Electronic Engineering, Faculty of Electrical and Electronic Engineering (FIEE)

Universidad Nacional del Callao (UNAC)

Bellavista, Callao, Peru

Email: enchavezg@unac.edu.pe

1. INTRODUCTION

The sequelae of COVID-19 can generate health complications, these are usually associated with changes in some physiological parameters of the human body that deviate from normal rates [1]. A significant proportion between 40% and 70% develop post-COVID-19 syndrome (PC19S) [2], which requires long-term longitudinal care for recovery. Despite the aforementioned, in some cases, hospital centers lack equipment that allows constant monitoring and requires medical personnel to manually measure vital signs at long random intervals, which does not allow detecting some anomalies in the readings, causing complications in patients with PC19S presenting with sequelae [3] such as dyspnea, which according to the research carried out by Goicochea-Ríos *et al.* [4] was the most frequent sequel with 84.4% and which can lead to the need for supplemental oxygen for persistent hypoxemia [5]. Another type of sequel is the cardiac one that has different magnitudes and implications for your health, sequels that can be tachycardia and heart palpitations [6].

Therefore, it is important to develop innovative and affordable platforms for remote monitoring of patients' biosignals during a healthcare crisis, which can be used from home [7] and that report valuable information about the patient's health status to hospitals [8]. Technological advances during the COVID-19 pandemic have led to the production of a plethora of new non-invasive devices for remote monitoring [9], such as the one developed by Idris *et al.* [10] that allowed remote monitoring of patients with COVID-19 through the oximeter reading sensor using the ESP32 MAX30100 web server that stores the information in the cloud. Other research developed by Wisana *et al.* [11] focused on creating a wearable so that the patient can monitor the beats per minute (BPM) and oxygen saturation (SpO₂) in real time, as well as provide notifications on smartphones and emails when the patient's condition is abnormal. Then the cases of people with PC19S began to increase, for which reason ambulatory monitoring of these patients began to be developed, such as that developed by Davies *et al.* [12] where great relevance was given to the non-invasive estimation of blood SpO₂ by pulse oximetry due to its clinical importance for the detection of sleep apnea and hypoxemia in the late post-infectious phase of COVID-19. Finally, Wu *et al.* [13] used a minicomputer and monitoring terminal to provide real-time updates on the physiological parameters of PC19S patients and provide early warning functions for medical personnel in case of emergency.

However, most of these devices focus mainly on the precision with which the biosignals are read or how interactive the platform where the biosignals are displayed is. Few studies focus on the use of geolocation and the sending of this information within alert messages, which becomes relevant when medical complications occur, especially in people with PC19S, of whom few studies focus despite being vulnerable and who are usually mobilizing in the rehabilitation stage. For this reason, in this research, a wearable was developed with the objective of monitoring the evolution of health and providing safety to patients with PC19S during the rehabilitation process using ESP32 to monitor their main biosignals for the control of their health, such as body temperature, SpO₂ and heart rate remotely using the internet of things (IoT) with an application developed with APP inventor on the cell phone and from the Firebase database or locally by viewing the measurement values on the light emitting diode (LCD) of the wearable. In addition, the wearable will immediately alert the medical center with an alert message containing the parameters of the biosignals and the current geolocation of the patient, if any abnormality is detected in the biosignals or if the emergency button of the application is pressed. This investigation is subdivided as follows: section 2, which deals with methods and materials, is focused on the assembly and operation of the wearable in conjunction with the mobile application. The section 3 presents the experimental procedure, where the cases and conditions in which the wearable will work to collect information are mentioned. The section 4 presents and discusses the results obtained when using the wearable with the experimental procedure. In section 5 is the conclusions of the main findings of this study, then there are the acknowledgments and finally the references.

2. MATERIALS AND METHODS

2.1. Materials

In Figure 1, it can be seen all the implemented components. An ESP32 microcontroller featuring a low-cost, low-power 32-bit system on chip (SoC), operating an ESPRESSIF-ESP32 chipset 240 MHz Xtensa® single/dual-core 32-bit LX6 microprocessor, with 4 MB quad serial peripheral interface (QSPI) flash, 520 kB static random access memory (SRAM), Bluetooth v4.2 and wireless fidelity (Wi-Fi) connectivity, operates with a voltage between 2.5 V and 3.6 V, this microcontroller is of Chinese origin [14], as can be seen in Figure 1(a). A Max30102 consisting of an optical module of 5.6 mm×3.3 mm×1.55 mm of 14 and with double wavelength LEDs, that is to say a light of 660 nm (red) and 880 nm (infrared) from China [15], as can be seen in Figure 1(b). A Max30205 sensor with an accuracy of 0.1 °C in the range of 37 to 39 °C and sending data through an inter-integrated circuit (I2C) compatible interface from the United States from the city of Minnesota [16], as can be seen in Figure 1(c). A 1.8-inch TFT-LCD (thin film transistor liquid crystal display) with a resolution of 128 by 160 pixels, as well as a micro-SD slot [17], as can be seen in Figure 1(d). A subscriber identity module SIM7600SA-H which is a multi-band area/global system for mobile communication (GSM)/general packet radio service (GRPS)/dual band long term evolution-frequency division duplexing (LTE-FDD)/evolved high-speed packet access (HSPA+)/time division synchronous code division multiple access (TD-SCDMA) module in a surface-mount technology (SMT) type. It has a robust extensibility with rich interfaces including UART, universal serial bus (USB2.zero), serial peripheral interface (SPI), I2C and general purpose input/output (GPIO) [18] from Shanghai City China provenance, as can be seen in Figure 1(e). A web development tool called MIT APP inventor, created by Massachusetts Institute of Technology, in which simple and complex applications can be created through mobile devices [19]. A lithium-ion NCR18650B battery with the capacity of 1,500 mAh from Japan [20], as can be seen in Figure 1(f). The TP4056 battery charger module not only allows you to charge the battery, but also maintain a stable current, this module is from China, as can be seen in Figure 1(g).

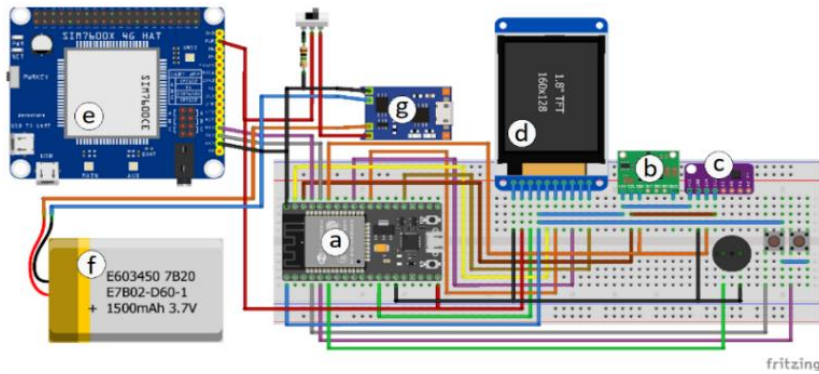


Figure 1. Circuit implementation: (a) ESP32, (b) MAX30102, (c) MAX30205, (d) 1.8-inch TFT-LCD, (e) SIM7600SA-H, (f) TP4056, and (g) NCR18650B

2.2. Equipment description

The ESP32 allows for easy IoT integration due to the native wireless modules, its use is therefore more appropriate considering the ease of development and use. The arduino integrated development environment (IDE) was used to program the ESP32, the board model was selected, adding a new library in board management [21]. The ESP32 connects device sensors and actuators via GPIO pins. EPS32 can communicate with other Wi-Fi and Bluetooth devices through its secure digital input/output (SPI/SDIO) or I2C/UART interfaces [22]. The two sensors, MAX30205 and MAX30102, are connected to an inter-integrated circuit (I2C) bus on the ESP32 that continuously receives data from all connected sensors, then processes the data and converts it to our known unit. All the sensor data will be sent to the user’s smartphone through a Bluetooth module of the ESP32 [23] that will display the values in the application. To facilitate the creation of mobile IoT applications, several visual components have been developed for a customized version of MIT APP inventor, as well as a set of extensions for its block-based programming language which allowed to design a fully functional application for smartphones [24]. In the event that any irregularity is detected in any of the health parameters, the ESP32 immediately activates an alert message through the global systems for mobile/general packet radio service (GSM/GPRS) device to a close relative or a doctor. In addition, the bracelet will have an alert button that, when pressed, will directly send an alert message to the mobile phone of the family, doctor or caregiver through the SIM7006SA-H regardless of the measurement parameters [25]. This general equipment description can be seen in Figure 2.

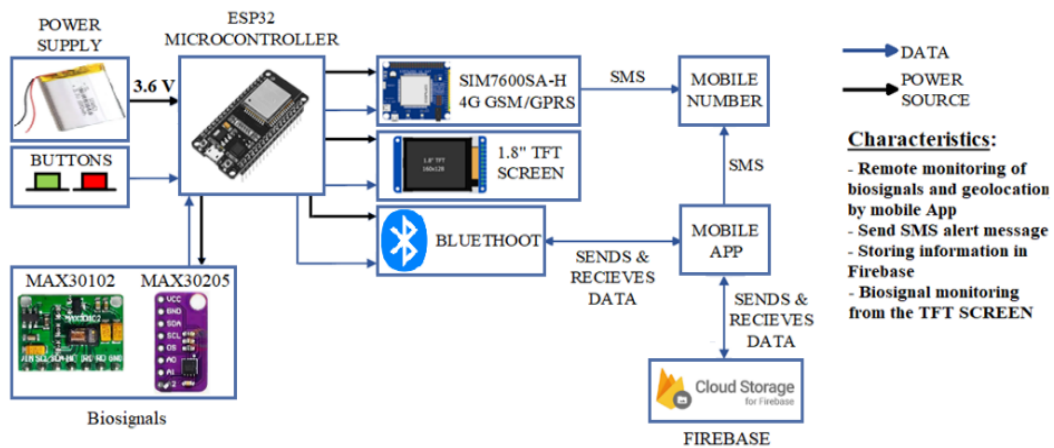


Figure 2. General system operation

2.2.1. Description of the operation of the equipment

The wearable initializes in the sensor stage where it collects the data and transforms it into a voltage variation that is then sent to the ESP32, once the data received on SpO₂, heartbeat, and temperature is in the ESP32 stage will be transformed into numerical data with its corresponding unit, once transformed into

numerical data it will be compared with the ranges that were established in the programming, in the case of heartbeats these ranges are based on the study of [26] where the non-diseasing heartbeat range is 60 to 100 times per minute, if the heart rate decreases, it is a heart attack called bradycardia or if it becomes faster, it means a tachycardia attack [27]. In the case of SpO₂, patient supervision must be strict, especially if therapeutic exercise is prescribed [28].

In this case, the permissible range of SpO₂ ≥92%, if it were lower after exercise, the patient’s admission to a hospital would be required and finally, a body temperature above 38°C indicates that there is a fever [29]. If the measurements obtained by the sensors are above or below these ranges, it is considered an anomaly that can cause damage to the health of the patient in the post-COVID-19 stage, if it is concluded that the measurement is not within within the normal ranges, this will activate a notification that will reach the application and the wearable to check the patient’s status if within the first 20 seconds this notification is not deactivated by pressing ok in the cell phone notification or by pressing a button that we will call “button of security” that is in the wearable within the first 20 seconds the alert message will be sent, this message contains the data of the temperature measurements, SpO₂, heart rate of the patient and their geolocation that will continue to be sent for 30 minutes in an interval of 5 minutes while notifying the patient that a message has been sent, the messaging system will be deactivated by pressing the security button at any time or once these 30 minutes have elapsed. After these 30 minutes, the consultation on the patient’s status is activated again, if the initial situation where the notification is not deactivated or the button is not pressed, it will be evaluated if there is position movement by means of global positioning system (GPS), if in If the GPS system detects that there is movement, it will limit itself to only displaying the values of the biosignals on the wearable Screen and in the application.

Another way to activate the alert messaging system independently of the biosignal measurements is by pressing the other button that we will call the emergency button that sends a message with the same content as mentioned above. All the measurements obtained in this stage will be encrypted and sent to the application stage. In the application stage, the person can register by placing their personal data such as names, surnames and ID where, once this information is received, it will be displayed on the cell phone screen, but prior to that, the person who is in the application will have a button that will It will allow synchronizing the Bluetooth of the cell phone with the Bluetooth of the ESP32. Once this connection is achieved, the measurements obtained by the ESP32 will be displayed on the cell phone screen, in case the alarm is activated and the security notification is displayed on the screen, this will not it will be silenced and will disappear until “ok” is pressed, which will allow the measurements that will be sent simultaneously to the cloud to continue being displayed. In the cloud stage the information will be stored and it can be reviewed remotely from any other device with internet, the information stored will be the patient’s data, their temperature, SpO₂, heartbeat and the coordinates of their location together with the time and date of that moment. The equipment operation flowchart can be seen in Figure 3.

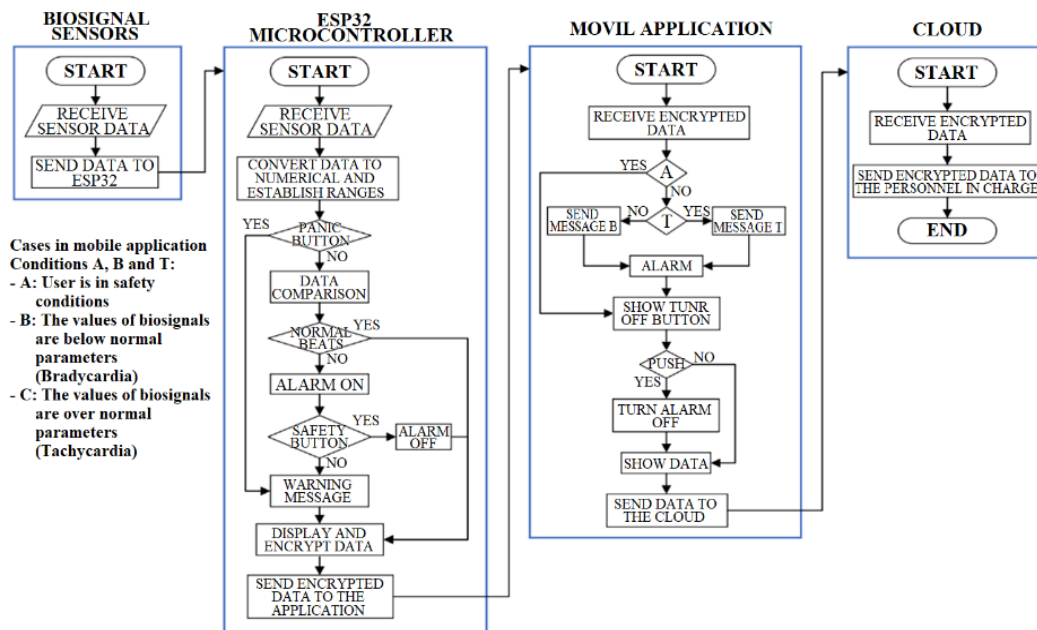


Figure 3. Flow chart of the system

2.3. Software analysis

The blocks in Figure 4 represents the programming of the Screen 1 (enter the personal data of the user). The blocks “ListPicker1” in the Figure 4(a) allows the users to select the bluetooth device to connect, being in this case the wearable of the article. The blocks in Figure 4(b) show the function “initialize global” that declares the variables to be sent to the wearable and the cloud. The block “Button1” in Figure 4(c) has the function to send these variables with the data entry values (name, surname, identity number, and age) packing it into a list to the wearable and cloud, this also confirms the wearable to start with the sensing of biosignals.

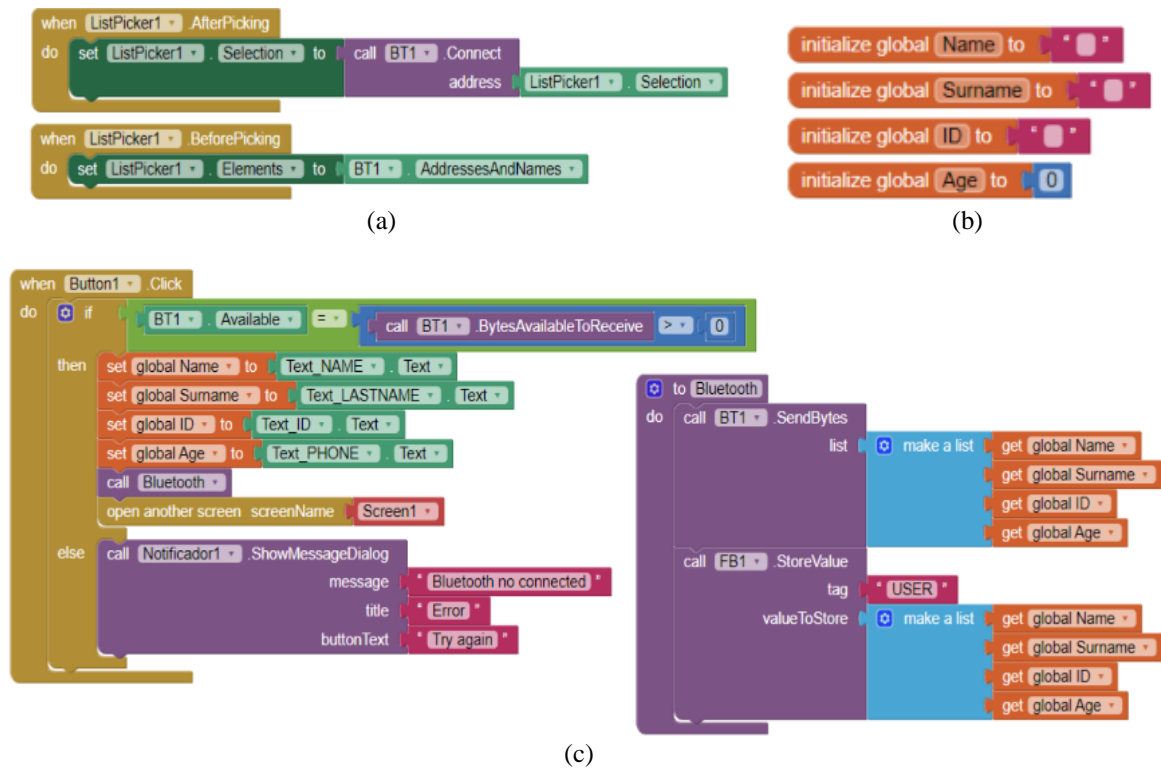


Figure 4. Programming the entry of personal data and verification of bluetooth connectivity (Screen 1): (a) selecting wearable, (b) declaration initial variables to send, and (c) sending the data to wearable and cloud

The blocks in Figure 5 represents the programming of the Screen 2 that captures instant values of biosignals and has also the option to return entry personal user data and the option to check graphs. The block “Clock1” in the Figure 5(a) allows capturing the biosignals instantly every minute by converting the bytes entered via bluetooth into a list to be interpretable in appinventor and displaying the biosignals of heart rate, SpO₂ and temperature in the graphical interface, as well as showing the location on a minimap of the interface. In case of anomaly, the cell phone will play an alert sound and call a notification to confirm if the user is in good conditions or not. It also seen two small blocks that have the function of changing the screen, being “CHANGE_DATA” the button to return to the user’s personal data entry Screen 1 in Figure 5(b) and “GRAPHS” to the graph Screen 3 with the biosignal data in Figure 5(c).

As can be seen in previous program figures, it was necessary to declare global variables to send and receive the same information to another Screen or signals device. To program the Screen for the graphs of heart rate, SpO₂ and temperature, the variables to be used for graphing must first be started as Figure 6 shows, in addition, this section captures not only the biosignals in real time, but also the location of the patient to subsequently send said data.

The blocks in Figure 7 captures all the biosignals and the user’s location. The “Collecting_data.Timer” block in the Figure 7(a) has the function of extracting the biosignals sent by the wearable via Bluetooth, unpacking all the sensed signals in a list including the state of the user analyzed by the wearable, the variables mentioned in Figure 6 are stored in this block. In the second block (LocationSensor1) in Figure 7(b), the geolocation data is captured to send these information to the cloud and the relative in case of alert.

(a)

(b)

(c)

Figure 5. Programming the extraction of biosignals instantly and alert message (Screen 2): (a) captures instant biosignals, (b) return to the entry personal data button, and (c) show graphs button

```

initialize global BT_GRAPHES to " "
initialize global LIST2 to " "
initialize global Domain to 0
initialize global Heart_Rate to 0
initialize global SPO2 to 0
initialize global Temperature to 0
initialize global Status to " "
initialize global Latitude to 0
initialize global Longitude to 0
    
```

Figure 6. Declaration of the variables to graph the biosignals and detect the user’s location (Screen 3)

(a)

(b)

Figure 7. Programming of the extraction of biosignals to be graphed and location of the user (Screen 3) (a) biosignal data capture and (b) geolocation data capture

The two blocks in the Figure 8 allow to establish limits to the graphs for a better interpretation of the biosignals, it is observed in the “Setting_graph_limit_x.Timer” block in the Figure 8(a) that the domain variable increases+1 (magnitude in minutes), this serves to later assign the domain of each sensed biosignal , while the “Setting_graph_limit_y.Timer” block in the Figure 8(b) the range of the ordinates is in a reasonable interval within human conditions.

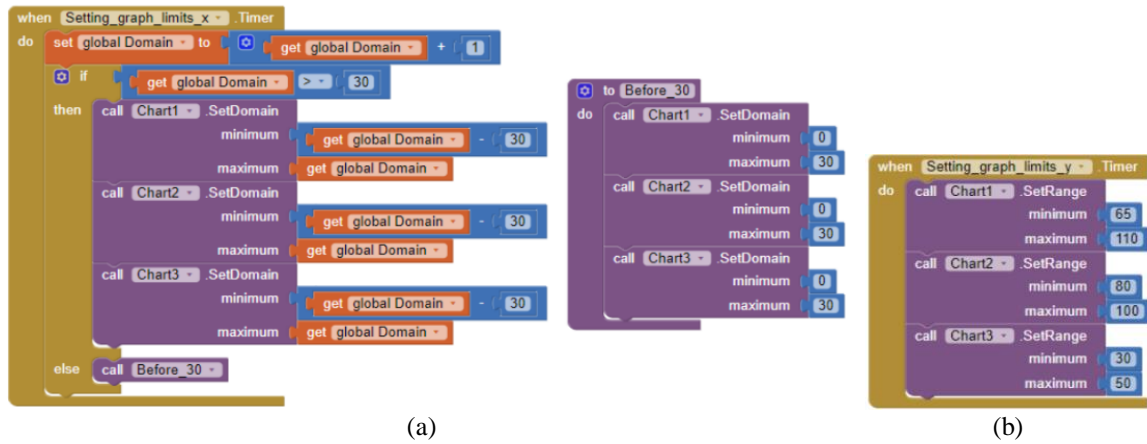


Figure 8. Programming of the declaration of limits of the graphs generated on the Screen (Screen 3)
 (a) set absic limits and (b) ordinates limits

Figure 9 show the functions to plot the biosignal entry data and the option to return to instant biosignal values Screen 2. The “Sending_data_to_the_cloud.Timer” block in the Figure 9(a) has the function to plot the data for its visualization, in addition to sending the biosignals and geolocation data to the Firebase cloud with its respective date, hour and minutes to have the aforementioned data recorded every minute. In the Firebase the geolocation will be sent as latitude and longitude. It also can be seen a “Button1” in Figure 9(b) button to change the visual on the user interface to instant biosignals values and position Screen 2.

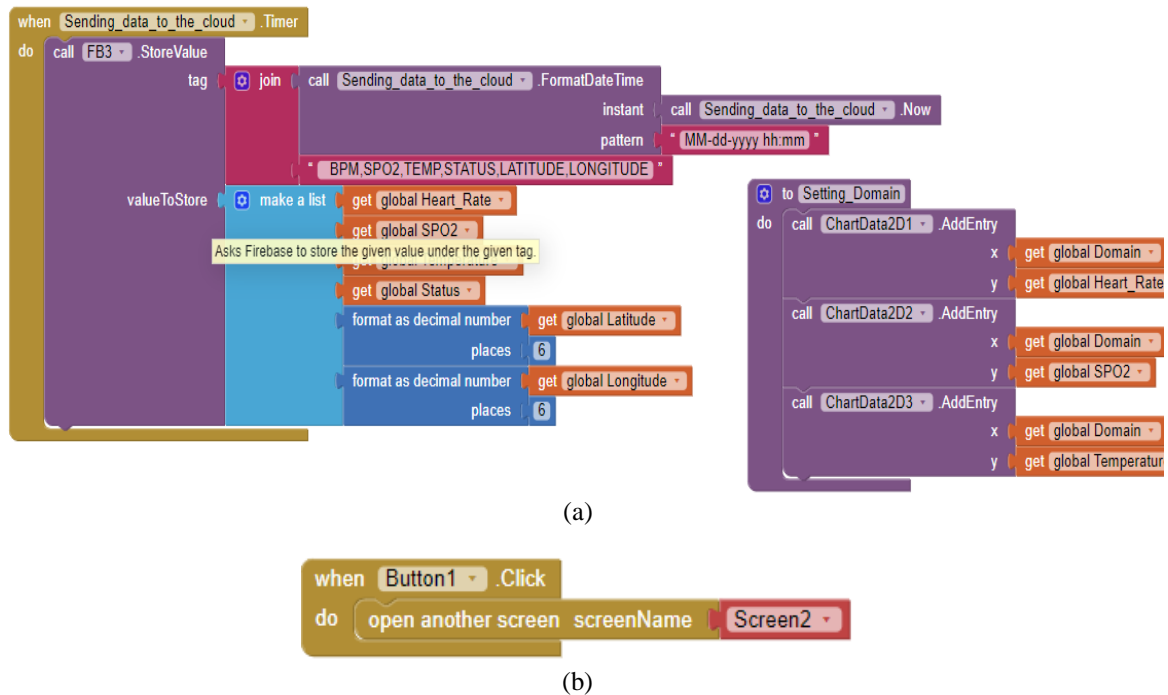


Figure 9. Programming to paint the biosignals on the graphs and sending the date, biosignals and location data to the cloud (Screen 3) (a) plotting biosignal data and (b) return to instant values interface

2.4. Experimental procedure

In order to carry out the tests, the patient was informed that the wereable had to be placed on the wrist. In order to measure the heart rate and SpO₂, the MAX30102 sensor will be placed on the index finger due to its large vasculature and the photoplethysmography (PPG) method will be used to measure the change in the absorbance ratio of red and infrared light, which can be estimate blood SpO₂ and heart rate [12], [30]. Many

investigators have investigated the reliability and validity of portable devices for monitoring biosignals in comparison with industrial equipment [31]. For this reason, the mean absolute error (MAE) (1), the relative error (2), the standard deviation (3) and standard error (4) were calculated in both devices for different exercise intensities. Once this stage was completed, the patient was asked to use the wearable until the battery ran out on 6 occasions and then the duration time of the battery in use was averaged and compared with the theoretical value using (5) [32] to verify if it complied with what was established in the autonomy time. In addition, taking into account the research carried out by Herscovici [33] where they use wireless network technologies in health centers to monitor their patients remotely from the cloud, a remote test was carried out with the patient wearing the wearable who performed a tour of a park for 30 minutes while the biosignal data and its geolocation were sent to the cloud from where the researchers could access it remotely to view the data obtained in firebase. Finally, it will activate the emergency button to verify the arrival of emergency messages for 15 minutes.

$$MAE = \frac{1}{n} \sum_{i=1}^n |y_i - \hat{y}_i| \quad (1)$$

where MAE is the mean absolute error, n is the number of samples, y_i and \hat{y}_i represent the measurement made by the industrial device and the one made by the wearable for the i th sample. It is very useful when it is required to measure the forecast error in the same units of the original series;

$$re_{err} = \frac{|True\ value - Measure\ Value|}{True\ value} \quad (2)$$

where re_{err} is the relative error, true value and measure value represent the calculated and actual values respectively, they can accurately reflect the credibility of a measurement [34]. This (3) will calculate the error that we make per unit of measurement of the measurements made by the wearable of each biosignal;

$$\sigma = \sqrt{\frac{\sum_{i=1}^N (x_i - \bar{x})^2}{N}} \quad (3)$$

where σ is the standard deviation, x is the variable, x_i as the observation number i of variable x , N number of observations and \bar{x} is the mean of the variable x . This (4) is useful if the values are close to the real measurements of the biosignals;

$$SE = \frac{\sigma}{\sqrt{n}} \quad (4)$$

where SE is the standard error and n is the number of samples. It is useful to use this equation to measure the spread of values in a data set, that is, it measures the variability of the sampling distribution, being in this case the measurement of the three biosignals;

$$T_1 = \frac{B_C}{C} \quad (5)$$

where B_C is the battery capacity in mAh and C is the total consumption of the device in mA, in order to obtain the time T_1 in hours, C must be considered as the total consumption in one hour. This equation reveals the theoretical performance of the wearable in each monitoring.

3. RESULTS AND DISCUSSION

3.1. Energy consumption

Considering that the wearable components are not constantly activated, there are two types of consumption, in active mode and sleep mode (SP), where in active mode the wearable consumes 144,524 mA and in SP mode it consumes 32,213 mA see Table 1. In order to find the consumption of the total current in one hour, we must make the sum of the current consumed in active mode multiplied by the time in active mode with the current consumed in SP mode multiplied by the time in SP mode in the interval of one hour, therefore, Table 1 is considered. The client was asked to perform 6 downloads for each monitoring interval of 60, 30, 15, 10, and 1 minutes to the wearable to calculate the autonomy time in each download using the values of Table 1 and (5) using a battery capacity of 1,500 mAh. The calculations of the battery autonomy are shown in Table 2 where it can be seen comparison of the theoretical duration of the battery and the actual duration of the battery.

With these results we can make the corresponding graphs that show us the comparison of theoretic and real duration of the wearable, these 6 graphs are shown in Figure 10. Figure 10(a) show the comparison of the

first six discharges between theoretic and real durations. Figure 10(b) show the comparison of the second six discharges between theoretic and real durations. Figure 10(c) show the comparison of the third six discharges between theoretic and real durations. Figure 10(d) show the comparison of the fourth six discharges between theoretic and real durations. Figure 10(e) show the comparison of the fifth six discharges between theoretic and real durations and Figure 10(f) show the comparison of the last six discharges between theoretic and real durations.

Table 1. Calculation of total current consumption in one hour

Interval for monitoring time (minutes)	Current consumption in active mode (mA)	Current consumption in SP mode (mA)	Time in active mode (seconds)	Time in SP mode (seconds)	Total current consumption in one hour (mA)
60	144.524	32.213	30	3,570	33,149
30			60	3,540	34,085
15			120	3,480	35,957
10			180	3,420	37,829
5			360	3,240	43,444
1			1,800	1,800	88,369

Table 2. Comparison of theoretical battery life and real battery life

Interval for monitoring time (minutes)	Theoric duration (h)	First discharge duration (h)	Second discharge duration (h)	Third discharge duration (h)	Fourth discharge duration (h)	Fifth discharge duration (h)	Sixth discharge duration (h)
60	45 h 15 m	42 h 52 m	41 h 58 m	41 h 42 m	41 h 13 m	40 h 55 m	40 h 52 m
30	44 m 01 m	41 h 36 m	40 h 32 m	39 h 58 m	39 h 23 m	39 h 06 m	39 h 08 m
15	44 m 43 m	39 h 28 m	38 h 09 m	37 h 28 m	37 h 35 m	36 h 59 m	37 h 04 m
10	39 h 12 m	37 h 45 m	36 h 52 m	36 h 38 m	36 h 40 m	36 h 37 m	36 h 26 m
5	34 h 31 m	32 h 32 m	31 h 46 m	31 h 31 m	31 h 18 m	31 h 16 m	31 h 09 m
1	16 h 59 m	15 h 53 m	15 h 35 m	15 h 28 m	15 h 16 m	15 h 15 m	15 h 12 m

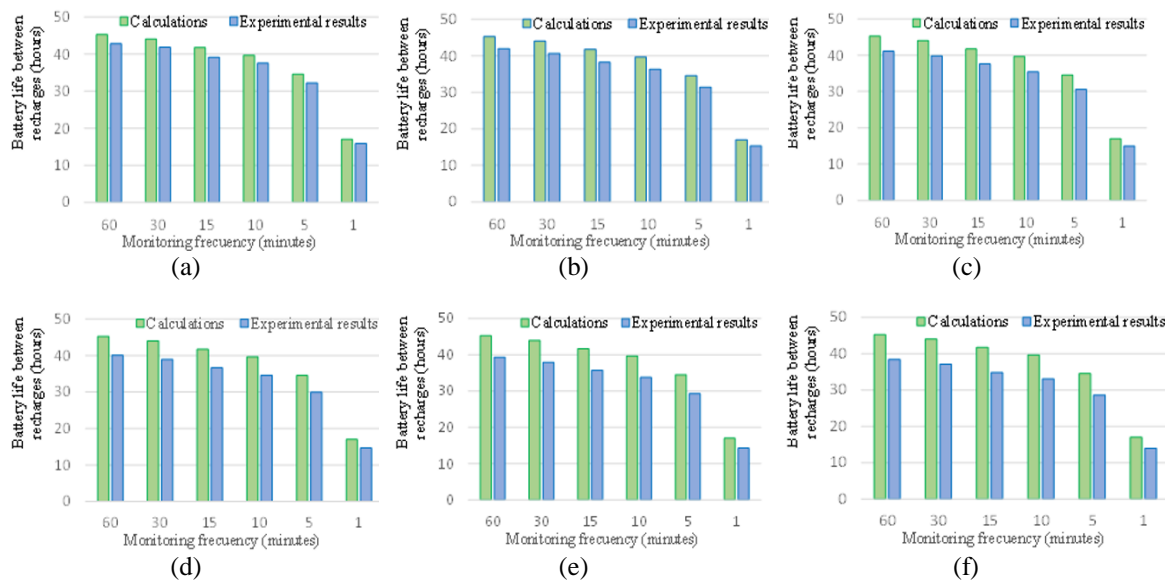


Figure 10. Graphs of the theoretical and actual discharge of the battery at each monitoring interval: (a) first 6 discharges, (b) second 6 discharges, (c) third 6 discharges, (d) fourth 6 discharges, (e) fifth 6 discharges, and (f) sixth 6 discharges

3.2. Using the graphical interface and FIREBASE database

The three screens in Figure 11 that must appear in order respecting the software procedure are displayed. On the “user data” Screen shown in Figure 11(a), the user’s personal data is entered, the Bluetooth device to be connected is selected by pressing the Bluetooth connection button and finally the SEND button sends this data to the wearable and to the cloud and takes us to the “instant values” Screen of Figure 11(b). On the “instant values” Screen you can see the heart rate, SpO₂ and temperature data instantly, you can also see the customer’s location by extracting the Google maps link, you can also see two buttons, the change data

button allows you to go to the previous screen to change or correct personal data and the view graphs button that takes us to the “graphs” screen in Figure 11(c) that practically shows us the graphs of these biosignals in a dynamic way, since the function charts 2D of the inventor app allows us to manipulate the range of the domain to be able to observe each sensed point more clearly. This Screen also contains a button that allows us to return to the “instant values” screen.

In Figure 12, we can observe the data that were extracted in the test, it can be seen the user’s personal data in a panoramic way. The three biosignals and the user’s condition collected from the wearable to the database through the mobile application that also sends geolocation data (latitude and length) packed in a list but easy to interpret. This data can be later exported to a JSON file, where it is possible to visualize all the data in a more dynamic way.

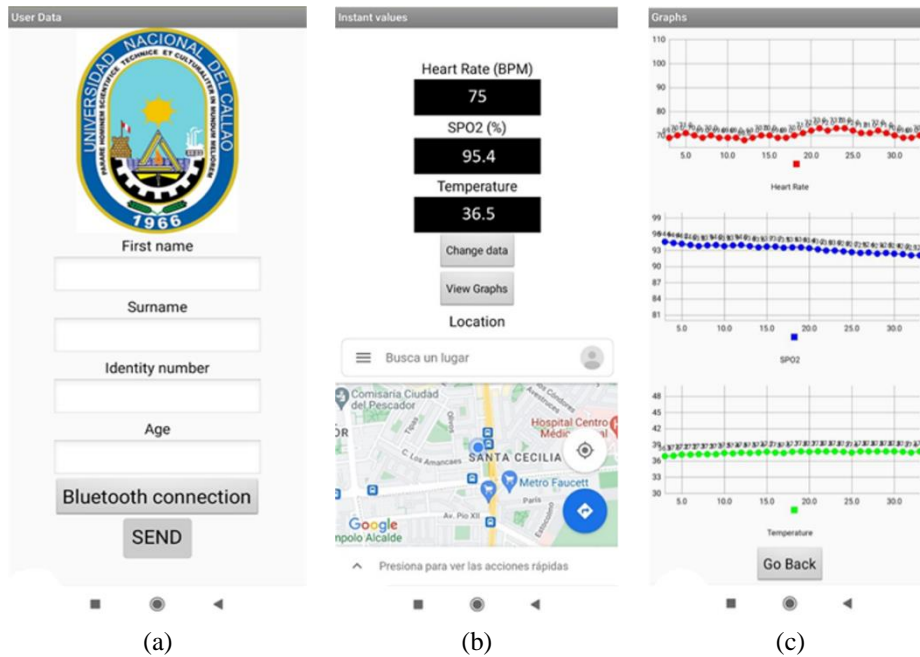


Figure 11. Graphical interface on the user’s mobile: (a) entry of personal data and selection of bluetooth device, (b) capture of instantaneous data of the biosignals and location of the user, and (c) graphs of biosignals

```

https://health-care-f4ac1-default-rtadb.firebaseio.com/
├── Health_care
│   └── USER: ["Ivan";"Muro Sanchez";"73273007";"32"]
└── values
    ├── 05-18-2023 01:00 BPM, SPO2, TEMP, STATUS, LATITUDE, LONGITUDE: ["69;94.6";"36.9";"NORMAL";"-12.060432";"-77.097892"]
    ├── 05-18-2023 01:01 BPM, SPO2, TEMP, STATUS, LATITUDE, LONGITUDE: ["70;94.4";"37.0";"NORMAL";"-12.060527";"-77.098142"]
    ├── 05-18-2023 01:02 BPM, SPO2, TEMP, STATUS, LATITUDE, LONGITUDE: ["71;94.2";"37.2";"NORMAL";"-12.060610";"-77.098258"]
    ├── 05-18-2023 01:03 BPM, SPO2, TEMP, STATUS, LATITUDE, LONGITUDE: ["70;94.0";"37.2";"NORMAL";"-12.060732";"-77.098216"]
    ├── 05-18-2023 01:04 BPM, SPO2, TEMP, STATUS, LATITUDE, LONGITUDE: ["69;93.8";"37.3";"NORMAL";"-12.060710";"-77.098149"]
    ├── 05-18-2023 01:05 BPM, SPO2, TEMP, STATUS, LATITUDE, LONGITUDE: ["70;93.9";"37.3";"NORMAL";"-12.060613";"-77.097967"]
    ├── 05-18-2023 01:06 BPM, SPO2, TEMP, STATUS, LATITUDE, LONGITUDE: ["69;94.0";"37.3";"NORMAL";"-12.060354";"-77.098205"]
    ├── 05-18-2023 01:07 BPM, SPO2, TEMP, STATUS, LATITUDE, LONGITUDE: ["69;93.8";"37.5";"NORMAL";"-12.060697";"-77.098107"]
    └── 05-18-2023 01:08 BPM, SPO2, TEMP, STATUS, LATITUDE, LONGITUDE: ["69;93.9";"37.4";"NORMAL";"-12.060601";"-77.098122"]
    
```

Figure 12. Storage of programmed data in the Firebase database

Personal data such as first and last name, instant biosignal data and geolocation data are also sent to the person in charge or the closest person via SMS. The particularity is that the geolocation data is sent with more detail for quick access to the user’s location as can be seen in Figure 13. A google map link is generated in which the current position of the user is reported just with the latitude and longitude variables captured by the wearable.

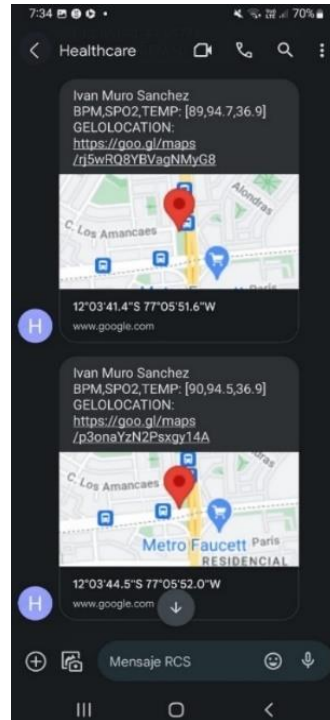


Figure 13. SMS messages sent being the wearable the sender and the person in charge the receiver

3.3. Data analysis

The biosignals through the wearable were considered as approximate values (Va), these data were compared with the measurement of commercial instruments, considering these measurements as the real values (Vr). That being said, we also consider the existence of measurement errors such as the absolute errors Ae and the relative error Re, we used (2) to calculate these errors. Besides, two states of the user have also been considered to measure the biosignals, being at rest and physical activity, this to verify the changes of the data received as can be seen in Tables 3 and 4 respectively.

Table 3. Theoretical and real values of the biosignals at rest

Heart rate (BPM)				Temperature (°C)				SpO ₂ level (%)			
Vr	Va	Ae	Re	Vr	Va	Ae	Re	Vr	Va	Ae	Re
86	85	1	1.176	36.8	36.9	0.1	0.271	95.6	95.8	0.2	0.209
85	86	1	1.163	36.9	36.9	0	0	95.7	95.6	0.1	0.105
85	84	1	1.190	37.1	36.9	0.2	0.542	95.4	95.7	0.3	0.313
86	85	1	1.176	37.0	37.2	0.2	0.538	95.4	95.5	0.1	0.105
87	86	1	1.163	36.9	37.1	0.2	0.539	95.2	95.2	0	0
87	86	1	1.163	37.1	36.9	0.2	0.542	95.0	95.3	0.3	0.315
86	86	0	0	37.1	36.9	0.2	0.542	95.1	94.8	0.3	0.316
85	84	1	1.190	37.0	37.0	0	0	95.0	94.7	0.3	0.317
85	84	1	1.190	37.2	37.2	0	0	94.9	95.2	0.3	0.315
83	83	0	0	37.1	37.1	0	0	94.9	94.7	0.2	0.211
85	86	1	1.163	37.1	37.2	0.1	0.269	94.7	94.7	0	0
85	86	1	1.163	37.4	37.4	0.2	0.535	94.8	94.6	0.2	0.211
86	86	0	0	37.1	37.1	0.1	0.270	94.7	94.4	0.3	0.318
84	83	1	1.205	37.3	37.3	0.2	0.536	94.6	94.9	0.3	0.316
83	84	1	1.190	37.1	37.1	0.1	0.270	94.6	94.8	0.2	0.211
82	81	1	1.235	37.1	37.1	0.1	0.270	94.7	94.7	0	0

When comparing the measurements obtained in the wearable with an oximeter, thermometer and commercial pulsometer, it was found that in the absolute error the highest value of SpO₂ is 0.3%, the temperature is 0.2 °C and the BPM is 1 in a state of rest and in the state of physical activity the maximum absolute error of SpO₂ is 0.6%, temperature 0.3% and BPM is 2. In the relative error the maximum value in the rest stage of SpO₂ is 0.318%, the temperature is 0.542% and BPM is 1.235%. While during physical activity the maximum relative error of SpO₂ is 0.645%, that of temperature is 0.824% and the BPM parameter has the largest error value of 2.299%.

Table 4. Theoretical and real values of the biosignals in physical activity

	Heart rate (BPM)				Temperature (°C)				SpO ₂ level (%)			
	Vr	Va	Ae	Re	Vr	Va	Ae	Re	Vr	Va	Ae	Re
85	85	0	0	36.2	36.3	0.1	0.276	95.2	95.7	0.5	0.525	
87	89	2	2.299	36.3	36.2	0.1	0.275	95.0	95.6	0.6	0.632	
90	88	2	2.222	36.4	36.1	0.3	0.824	94.6	95.2	0.6	0.634	
93	92	1	1.075	36.4	36.1	0.3	0.824	94.7	94.6	0.1	0.106	
93	92	1	1.075	36.5	36.7	0.2	0.548	94.3	94.3	0	0	
95	93	2	2.105	36.5	36.5	0	0	94.1	94.0	0.1	0.106	
96	96	0	0	36.6	36.6	0	0	94.1	94.3	0.2	0.213	
98	97	1	1.020	36.6	36.4	0.2	0.546	93.9	93.5	0.4	0.426	
98	97	1	1.020	36.5	36.2	0.3	0.822	93.7	93.7	0	0	
101	102	1	0.990	36.6	36.4	0.2	0.546	93.8	94.0	0.2	0.213	
101	99	2	1.980	36.6	36.6	0	0	93.3	93.6	0.3	0.322	
101	99	2	1.980	36.6	36.4	0.2	0.546	93.2	92.8	0.4	0.429	
102	103	1	0.980	36.7	36.5	0.2	0.545	93.2	92.6	0.6	0.644	
104	103	1	0.962	36.7	36.9	0.2	0.545	93.0	93.6	0.6	0.645	
106	105	1	0.943	36.8	36.7	0.1	0.272	92.9	93.4	0.5	0.538	
108	106	2	1.852	37	36.7	0.3	0.811	92.8	93.1	0.3	0.323	

We can make the graphs of each biosignal shown in Tables 3 and 4 and observe the difference between the value measured from a commercial device and the wearable when the user is at rest or in physical activity, as can be seen in Figure 14. Figure 14(a) show the comparison between theoretic and real values of heart rate on rest. Figure 14(b) show the comparison between theoretic and real values of heart rate on physical activity. Figure 14(c) show the comparison between theoretic and real values of temperature on rest. Figure 14(d) show the comparison between theoretic and real values of temperature on physical activity. Figure 14(e) show the comparison between theoretic and real values of SpO₂ on rest and Figure 14(f) show the comparison between theoretic and real values of SpO₂ on physical activity.

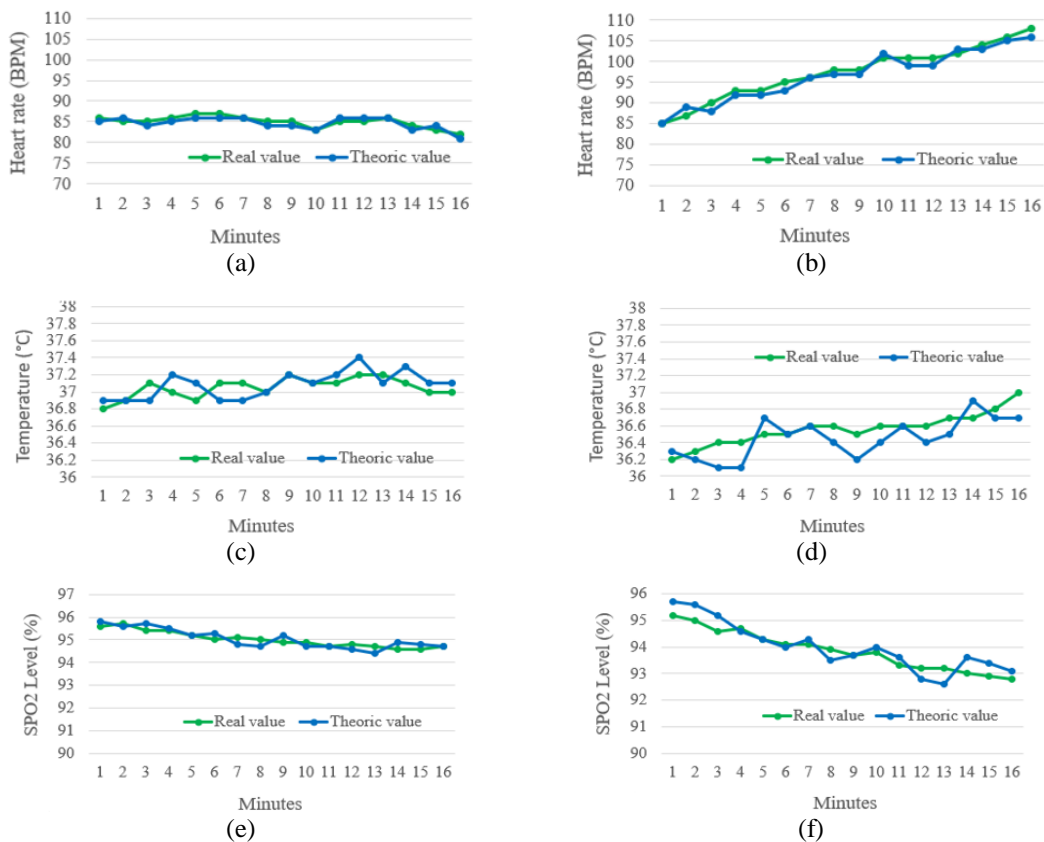


Figure 14. Graphs of the values of the biosignals of the commercial device and the wearable: (a) heart rate on rest, (b) heart rate in physical activity, (c) temperature on rest, (d) temperature in physical activity, (e) SpO₂ on rest, and (f) SpO₂ in physical activity

The (3) and (4) are used to find the standard deviation and the standard error. Wich are considered to verify the progressive change of the data, as shown in Table 5 and the MAE with (1) to verify if the aforementioned conditions affect the sensing accuracy as shown in Table 6. It is worth mentioning that this article will focus more on the measurements of biosignals and their accuracy.

Table 5. Standard deviation and standar error of biosignals

Biosignal	Standart deviation				Standard error			
	Resting		Physical activity		Resting		Physical activity	
	Vr	Va	Vr	Va	Vr	Va	Vr	Va
Heart rate	1.4142	1.4930	6.6017	6.3442	0.3535	0.3732	1.6504	1.5860
Temperature	0.1154	0.1558	0.1927	0.2365	0.0288	0.0389	0.0481	0.0591
SpO ₂	0.3525	0.4364	0.7597	0.9186	0.0881	0.1091	0.1899	0.2296

From the results an acceptable level of precision is obtained in heart rate and temperature with a standard error of 1.5860 and 0.0591 respectively in comparison with the values obtained by Sakphrom *et al.* [7] where a standard error of 1.22 was obtained in the measurement of the frequency. heart rate and 0.13 in body temperature. We noticed that the wearable has a better precision when measuring body temperature. Regarding the precision when measuring SpO₂ in the research carried out by Syaifudin *et al.* [35], the standard deviation of the highest value obtained was 0.87, which indicates a lower precision than the wearable, which obtained a standard deviation of 0.4364.

Table 6. Mean absolute error of biosignals

Biosignal	MAE	
	Resting	Physical activity
Heart rate	0.8125	1.2500
Temperature	0.1186	0.1675
SpO ₂	0.1936	0.3375

Regarding the technologies that remotely alert any anomaly in the measurement of biosignals, the research of Narvaez *et al.* [32] is cited, who used the API Twilio5 to send alert messages, a page that provides various services for sending SMS, voice and notifications through the web, which could cause problems if the monitoring is to be carried out outside the home. On the other hand, the developed wearable has an application that allows monitoring for outpatients that sends the measurements of biosignals and geolocation in the alert message, having greater flexibility in the doctor’s interpretation of the situation and in the space that the wearable can be used by people who follow a rehabilitation program.

4. CONCLUSION

This system is flexible and efficient. The app works on smartphones. In addition to the sensors, the GSM module and ESP32 are integrated with Wi-Fi and Bluetooth modules, making it small and light allowing monitoring anytime anywhere. In addition, it can facilitate the management of databases through the cloud and safely and immediately communicate any anomaly that occurs with an alert message that contains geolocation. When observing the standard deviation of the wearable measurements in the different stages of activity, we notice that the standard deviation of heart rate, temperature and SpO₂ in the resting stage is equal to 1.4930, 0.1154 and 0.3525 respectively, it is lower in comparison with the means carried out in the physical activity stage where the standard deviation in heart rate, temperature and saturation was 6.3442, 0.2365 and 0.9186 respectively. For this reason, it is concluded that the error in the mediations increases when the person performs physical activity, this is since the person is in motion, which destabilizes the contact of the sensors with the patient and that when perspiring a change is generated in the electrical conductance of the skin. It was concluded that the duration of the battery varied with respect to the number of readings per hour, in the case of 1 reading per hour the System consumed 33,149 mA and the battery had a theoretical duration of 45 h and 15 m while when 60 readings were performed per hour, a consumption of 88,369 mA was obtained and the battery had a theoretical duration of 16 h and 59 m, which indicates that the greater the number of readings, the greater the energy consumption and the shorter the battery life.

ACKNOWLEDGEMENTS

We thank Universidad Nacional del Callao and the Research Vice President for their support, guidance and motivation to conduct scientific research.

REFERENCES

- [1] A. I. Siam *et al.*, “Secure health monitoring communication systems based on IoT and cloud computing for medical emergency applications,” *Computational Intelligence and Neuroscience*, vol. 2021, 2021, doi: 10.1155/2021/8016525.
- [2] M. Z. Yan, M. Yang, and C.-L. Lai, “Post-COVID-19 syndrome comprehensive assessment: from clinical diagnosis to imaging and biochemical-guided diagnosis and management,” *Viruses*, vol. 15, no. 2, p. 533, Feb. 2023, doi: 10.3390/v15020533.
- [3] K. K. B. Cardins, S. A. da C. Uchôa, L. V. e. Oliveira, and C. H. S. de M. Freitas, “Care of people with Post-COVID-19 sequelae in the scope of primary health care: scoping review protocol,” *International Journal of Environmental Research and Public Health*, vol. 19, no. 21, p. 13987, Oct. 2022, doi: 10.3390/ijerph192113987.
- [4] E. D. S. Goicochea-Ríos, O. M. C. Paz-Soldán, N. I. Gómez-Goicochea, and J. Vicuña-Villacorta, “Post-infection sequelae by COVID 19 in patients at Hospital I Florencia de Mora. Trujillo, Peru,” *Revista de la Facultad de Medicina Humana*, vol. 22, no. 1, pp. 754–764, Sep. 2022, doi: 10.25176/RFMH.v22i4.5045.
- [5] C. A-C. Malvaéz, A. Galván-Lobato, and M. Ortíz-Benavides, “Design of a pulse oximeter with altitude measurement bluetooth communication and android application,” *PriMera Scientific Engineering*, vol. 1, no. 3, pp. 2–15, Nov. 2022, doi: 10.56831/PSEN-01-014.
- [6] C. R. Márquez, E. F. C. Saavedra, and C. R. M. U. C. Vallejo-Perú, “Long-term post-COVID-19 sequelae. a review study (in spanish: secuelas pos-COVID-19 a largo plazo. Un estudio de revisión),” *MediSur*, vol. 20, no. 4, pp. 733–744, 2022.
- [7] S. Sakphrom, T. Limpitit, K. Funsian, S. Chandhaket, R. Haiges, and K. Thinsurat, “Intelligent medical system with low-cost wearable monitoring devices to measure basic vital signals of admitted patients,” *Micromachines*, vol. 12, no. 8, pp. 1–17, 2021, doi: 10.3390/mi12080918.
- [8] N. Chinnamatha, R. Z. Ahmed, and K. Kalegowda, “Development of health monitoring system using smart intelligent device,” *Indonesian Journal of Electrical Engineering and Computer Science*, vol. 28, no. 3, pp. 1381–1387, Dec. 2022, doi: 10.11591/ijeecs.v28.i3.pp1381-1387.
- [9] A. B. Gala, M. T. B. Pope, M. Leo, T. Lobban, and T. R. Betts, “NICE atrial fibrillation guideline snubs wearable technology: a missed opportunity?,” *Clinical Medicine, Journal of the Royal College of Physicians of London*, vol. 22, no. 1, pp. 77–82, 2022, doi: 10.7861/clinmed.2021-0436.
- [10] S. K. Idris, M. H. A. Zulkifli, H. Haroon, H. A. Razak, and A. S. M. Zain, “Health monitoring system with internet of things implementation,” in *Proceedings of 4th International Conference on Telecommunication, Electronic and Computer Engineering (ICTEC'22)*, 2022, p. 2.
- [11] I. D. G. H. W. Wisana, P. C. Nugraha, F. Amrinsani, F. F. Sani, Y. I. Anwar, and S. Palanisamy, “Smartband for heartbeat and oxygen saturation monitoring with critical warning to paramedic via IoT,” *Jurnal Teknokes*, vol. 15, no. 3, pp. 161–166, 2022, doi: 10.35882/teknokes.v15i3.317.
- [12] H. J. Davies, I. Williams, N. S. Peters, and D. P. Mandic, “In-ear spo2: a tool for wearable, unobtrusive monitoring of core blood oxygen saturation,” *Sensors (Switzerland)*, vol. 20, no. 17, pp. 1–12, 2020, doi: 10.3390/s20174879.
- [13] J.-Y. Wu, Y. Wang, C. T. S. Ching, H.-M. D. Wang, and L.-D. Liao, “IoT-based wearable health monitoring device and its validation for potential critical and emergency applications,” *Frontiers in Public Health*, vol. 11, no. June, pp. 1–13, 2023, doi: 10.3389/fpubh.2023.1188304.
- [14] A. Paziienza and D. Monte, “Introducing the monitoring equipment mask environment,” *Sensors*, vol. 22, no. 17, pp. 0–15, 2022, doi: 10.3390/s22176365.
- [15] S. Valenti *et al.*, “Wearable multisensor ring-shaped probe for assessing stress and blood oxygenation: design and preliminary measurements,” *Biosensors*, vol. 13, no. 4, 2023, doi: 10.3390/bios13040460.
- [16] D. Asiain, J. Ponce de León, and J. R. Beltrán, “MsWH: a multi-sensory hardware platform for capturing and analyzing physiological emotional signals,” *Sensors*, vol. 22, no. 15, pp. 1–25, 2022, doi: 10.3390/s22155775.
- [17] M. Noguera, B. Millán, J. J. Pérez-Paredes, J. M. Ponce, A. Aquino, and J. M. Andújar, “A new low-cost device based on thermal infrared sensors for olive tree canopy temperature measurement and water status monitoring,” *Remote Sensing*, vol. 12, no. 4, 2020, doi: 10.3390/rs12040723.
- [18] I. Potamitis, I. Rigakis, N. A. Tatlas, and S. Potirakis, “In-vivo vibroacoustic surveillance of trees in the context of the IoT,” *Sensors (Switzerland)*, vol. 19, no. 6, pp. 1–14, 2019, doi: 10.3390/s19061366.
- [19] D. A. Angamarca-Avenidaño, J. F. Saquicela-Moncayo, B. H. Capa-Carrillo, and J. C. Cobos-Torres, “Charge equalization system for an electric vehicle with a solar panel,” *Energies*, vol. 16, no. 8, 2023, doi: 10.3390/en16083360.
- [20] D. Wang, Y. Bao, and J. Shi, “Online lithium-ion battery internal resistance measurement application in state-of-charge estimation using the extended kalman filter,” *Energies*, vol. 10, no. 9, 2017, doi: 10.3390/en10091284.
- [21] A. C. da Silva, W. de S. Rodrigues, B. P. Gonçalves, M. A. da Cruz, R. P. Gomes, and D. B. de Alencar, “Locator bracelet with QR code for elderly people with Alzheimer’s,” *International Journal of Advanced Engineering Research and Science*, vol. 7, no. 6, pp. 81–86, 2020, doi: 10.22161/ijaers.76.10.
- [22] M. M. Islam, A. Rahaman, and M. R. Islam, “Development of smart healthcare monitoring system in IoT environment,” *SN Computer Science*, vol. 1, no. 3, 2020, doi: 10.1007/s42979-020-00195-y.
- [23] N. A. Jasman, M. F. I. M. Jalil, A. Mukhtar, K. S. M. Sahari, and M. E. Rusli, “IoT-based obstacle detection system for visually impaired person with smartphone module,” *Journal of Advances in Information Technology*, vol. 13, no. 4, pp. 368–373, 2022, doi: 10.12720/jait.13.4.368-373.
- [24] A. A. Mustofa, Y. A. Dagnew, P. Gantela, and M. J. Idrisi, “SECHA: a smart energy-efficient and cost-effective home automation system for developing countries,” *Journal of Computer Networks and Communications*, vol. 2023, 2023, doi: 10.1155/2023/8571506.
- [25] E. Kałamajska, J. Misiurewicz, and J. Weremczuk, “Wearable pulse oximeter for swimming pool safety,” *Sensors*, vol. 22, no. 10, 2022, doi: 10.3390/s22103823.
- [26] P. Peris-Lopez, L. González-Manzano, C. Camara, and J. M. de Fuentes, “Effect of attacker characterization in ECG-based continuous authentication mechanisms for internet of things,” *Future Generation Computer Systems*, vol. 81, pp. 67–77, 2018, doi: 10.1016/j.future.2017.11.037.

- [27] K. Rawal and G. Gabrani, "Healthcare smartwatch for monitoring elderly," *International Journal of Innovative Technology and Exploring Engineering*, vol. 9, no. 2, pp. 737–741, 2019, doi: 10.35940/ijitee.b6834.129219.
- [28] A. Arbillaga-Etxarri *et al.*, "Respiratory physiotherapy in post-COVID-19: a decision-making algorithm for clinical practice," *Open Respiratory Archives*, vol. 4, no. 1, 2022, doi: 10.1016/j.opresp.2021.100139.
- [29] I. Gorczewska, A. Szurko, A. Kielboń, A. Stanek, and A. Cholewka, "Determination of internal temperature by measuring the temperature of the body surface due to environmental physical factors-first study of fever screening in the COVID pandemic," *International Journal of Environmental Research and Public Health*, vol. 19, no. 24, 2022, doi: 10.3390/ijerph192416511.
- [30] B. J. Singstad *et al.*, "Estimation of heart rate variability from finger photoplethysmography during rest, mild exercise and mild mental stress," *Journal of Electrical Bioimpedance*, vol. 12, no. 1, pp. 89–102, 2021, doi: 10.2478/JOEB-2021-0012.
- [31] W. Te Ho, Y. J. Yang, and T. C. Li, "Accuracy of wrist-worn wearable devices for determining exercise intensity," *Digital Health*, vol. 8, 2022, doi: 10.1177/20552076221124393.
- [32] R. B. Narvaez, D. M. Villacis, T. M. Chalen, and W. Velasquez, "Heart rhythm monitoring system and IoT device for people with heart problems," in *2017 International Symposium on Networks, Computers and Communications (ISNCC)*, 2017, doi: 10.1109/ISNCC.2017.8072004.
- [33] N. Herscovici *et al.*, "m-health e-emergency systems: Current status and future directions," *IEEE Antennas and Propagation Magazine*, vol. 49, no. 1, pp. 216–231, 2007, doi: 10.1109/MAP.2007.371030.
- [34] B. Zhang, H. Ren, G. Huang, Y. Cheng, and C. Hu, "Predicting blood pressure from physiological index data using the SVR algorithm 08 information and computing sciences 0801 artificial intelligence and image processing," *BMC Bioinformatics*, vol. 20, no. 1, pp. 1–15, 2019, doi: 10.1186/s12859-019-2667-y.
- [35] S. Syaifudin, T. Triwiyanto, D. A. Harditamara, and F. Masood, "Pulse oximeter design for SpO2 and BPM recording on external memory to support the Covid-19 diagnosis," *Jurnal Teknokes*, vol. 15, no. 3, pp. 147–153, 2022, doi: 10.35882/teknokes.v15i3.303.

BIOGRAPHIES OF AUTHORS



Dr. Santiago Linder Rubiños Jimenez    is Doctor in Electrical Engineering, Master in Electrical Engineering with a mention in Management of Electrical Energy Systems, Bachelor of the professional career in electrical engineering. He was graduate with work experience in the area of teaching, engineering projects and research. He was Master in Electrical Engineering. He can be contacted at email: slrubinosjh@unac.edu.pe.



MSc. Mario Alberto Garcia Perez    is University Professor at the "National University of Callao" and the "Universidad Nacional Mayor de San Marcos", Engineer in Fluid Mechanics with a master's degree in hydraulics from the "National University of Engineering" and educational management from the "Technological University of Peru" with research in the area of irrigation and drainage works in the Ministry of Agriculture of Peru. He can be contacted at email: magarciap@unac.edu.pe.



Eng. Eduardo Nelson Chavez Gallegos    is Electronic Engineer with a master's degree in biomedicine, he founded the IoT UNAC branch in the Faculty of Electrical and Electronic Engineering (FIEE) in Universidad Nacional del Callao (UNAC). He is a member of the research area of the vice-rectorate. He can be contacted at email: enchavezg@unac.edu.pe.



Dra. Linett Angélica Velasquez Jimenez    is a Dra. in administration in Univerisidad Nacional del Callao. M.Sc. in Quality and Productivity Management, Industry Engineer. She has worked on quality management issues in process improvement, as well as safety and health at work. She can be contacted at email: lavelasquezjh@unac.edu.pe.



MSc. Niko Alain Alarcon Cueva    is an M.Sc. in Electric Engineer, Speciality: with a mention in Electrical Power Systems Management. He has held various positions that have allowed him to manage human capital within the teams in which he has participated. He can be contacted at email: naalarconct@unac.edu.pe.



Dr. Mauro Bernardo Sanchez Cabrera    is a University Professor of the Faculty of Electrical and Electronic Engineering of the National University of Callao, Former Director of the Research Institute of the Faculty of Electrical and Electronic Engineering of the National University of Callao with a master's degree in Civil and Commercial Law. He can be contacted at the email: mbsanchezc@unac.edu.pe.